Light Harvesting and Energy Transfer in Laser−Dye-Labeled Poly(aryl ether) Dendrimers

Alex Adronov, Sylvain L. Gilat,† Jean M. J. Fréchet,* Kaoru Ohta, Frederik V. R. Neuwahl,‡ and Graham R. Fleming

Contribution from the Department of Chemistry, University of California, Berkeley, 94720-1460

Received September 8, 1999. Revised Manuscript Received November 22, 1999

Abstract: The photophysical properties of a series of laser−dye-labeled poly(aryl ether) dendrimers, generations 1−4, have been determined. The dendrimers act as extremely efficient light-harvesting antennae capable of transferring light energy through space from their periphery to their core. The light-harvesting ability of these molecules increases with generation due to an increase in the number of peripheral chromophores. The energy-transfer efficiency was found to be quantitative for generations 1−3, with only a slight decrease observed for the fourth generation (∼93%). Due to the high extinction coefficients and fluorescence quantum yields of the chromophores and the efficient intramolecular energy transfer of the dendritic assemblies, these macromolecules have the potential to become integral components of molecular photonic devices.

Introduction

In natural photosynthetic systems, a large array of chlorophyll molecules surrounds a single reaction center.[1] The intricate chlorophyll assembly acts as an efficient light-harvesting antenna that captures photons from the sun and transfers their energy to the reaction center where it is utilized to induce a charge separation and the eventual formation of ATP.[2] Interestingly, the energy of any photon absorbed anywhere in this relatively large assembly of chromophores is passed rapidly to the reaction center with greater than 90% efficiency over nanometer distances.[3] It is clear that artificial light-harvesting systems capable of converting solar radiation into a useful source of fuel with similar efficiencies would be extremely beneficial.[4] Recognizing this fact, a wide variety of organic,[5] organometallic,[6] supramolecular,[7] polymeric,[8] and dendritic[9] chromophore assemblies have been developed to mimic the natural light-harvesting machinery.

Several groups have prepared polymeric light-harvesting systems in which chromophores and quenchers were incorporated into a linear polymer.[8] These linear structures exhibit moderate energy-transfer efficiencies (20−70%), and the in-

* Author to whom correspondence should be addressed: (phone) (510) 643-3077; (fax) 643-3079; (e-mail) frechet@cchem.berkeley.edu.

† Current address: Bell Laboratories, 600 Mountain Ave., Room 1D-246, Murray Hill, NJ 07974; (phone) (908) 582-4604; (fax) (908) 582-3609; (e-mail) sgilat@bell-labs.com.

‡ Current address: Department of Chemistry and LENS, University of Florence, Italy.

(1) (a) McDermott, G.; Prince, S. M.; Freer, A. A.; Hawthornthwaite-Lawless, A. M.; Papiz, M. Z.; Cogdell, R. J.; Isaacs, N. W. *Nature* **1995**, *374*, 517−521. (b) Kühlbrandt, W.; Wang, D. N. *Nature* **1991**, *350*, 130−134. (c) Kühlbrandt, W.; Wang, D. N.; Fujiyoshi, Y. *Nature* **1994**, 614−621. (d) Kühlbrandt, W. *Nature* **1995**, *374*, 497−498.

(2) Lehninger, A. L.; Nelson, D. L.; Cox, M. M. *Principles of Biochemistry*; Worth Publishers Inc.: New York, 1993; pp 571−591.

(3) Glazer, A. N. *Annu. Rev. Biophys. Biophys. Chem.* **1995**, *14*, 47−77.

(4) Grätzel, M., Ed. *Energy Resources through Photochemistry and Catalysis*; Academic Press: New York, 1983.

(5) (a) Berberan-Santos, M. N.; Pouget, J.; Valeur, B.; Canceill, J.; Jullien, L.; Lehn, J.-M. *J. Phys. Chem.* **1993**, *97*, 11376−11379. (b) Jullien, L.; Canceill, J.; Valeur, B.; Bardez, E.; Lehn, J.-M. *Angew. Chem., Int. Ed. Engl.* **1994**, *33*, 2438−2439. (c) Jullien, L.; Canceill, J.; Valeur, B.; Bardez, E.; Lefèvre, J.-P.; Lehn, J.-M.; Marchi-Artzner, V.; Pansu, R. *J. Am. Chem. Soc.* **1996**, *118*, 5432−5442. (d) Wang, P. F.; Valeur, B.; Filhol, J.-S., Canceill, J.; Lehn, J.-M. *New J. Chem.* **1996**, *20*, 895−907. (e) Paddon-Row: M. N. *Acc. Chem. Res.* **1994**, *27*, 18−25. (f) Clayton, A. H. A.; Scholes, G. D.; Ghiggino, K. P.; Paddon-Row, M. N. *J. Phys. Chem.* **1996**, *100*, 10912−10918. (g) Stewart, G. M.; Fox, M. A. *J. Am. Chem. Soc.* **1996**, *118*, 4354−4360. (h) Beggren, M.; Dodabalapur, A.; Slusher, R. E.; Bao, Z. *Nature* **1997**, *389*, 466−469. (i) Vollmer, M. S.; Würthner, F.; Effenberger, F.; Emele, P.; Meyer, D. U.; Stümpfig, T.; Port, H.; Wolf, H. C. *Chem. Eur. J.* **1998**, *4*, 260−269. (j) Kawahara, S.; Uchimaru, T.; Murata, S. *Chem. Commun.* **1999**, 563−564. (k) Gust, D.; Moore, T. A.; Moore, A. L. *Acc. Chem. Res.* **1993**, *26*, 198−205. (l) Steinberg-Yfrach, G.; Liddell, P. A.; Hung, S.-C.; Moore, A. L.; Gust, D.; Moore, T. A. *Nature* **1997**, *385*, 239−241.)m) Steinberg-Yfrach, G.; Rigaud, J.-L.; Durantini, E. N.; Moore, A. L.; Gust, D.; Moore, T. A. **1998**, *392*, 479−482.

(6) (a) Seth, J.; Palaniappan, V.; Johnson, T. E.; Prathapan, S.; Lindsey, J. S.; Bocian, D. F. *J. Am. Chem. Soc.* **1994**, *116*, 10578−10592. (b) Wagner, R. W.; Johnson, T. E., Lindsey, J. S. *J. Am. Chem. Soc.* **1996**, *118*, 11166−11180. (c) Hsiao, J.-S.; Krueger, B. P.; Wagner, R. W.; Johnson, T. E.; Delaney, J. K.; Mauzerall, D. C.; Fleming, G. R.; Lindsey, J. S.; Bocian, D. F.; Donohoe, R. J. *J. Am. Chem. Soc.* **1996**, *118*, 11181−11193. (d) Seth, J.; Palaniappan, V.; Wagner, R. W.; Johnson, T. E.; Lindsey, J. S.; Bocian, D. F. *J. Am. Chem. Soc.* **1996**, *118*, 11194−11207. (e) Strachan, J.-P.; Gentemann, S.; Seth, J.; Kalsbeck, W. A.; Lindsey, J. S.; Holten, D.; Bocian, D. F. *J. Am. Chem. Soc.* **1997**, *119*, 11191−11201. (f) Li, F.; Yang, S. I.; Ciringh, Y.; Seth, J.; Martin, C. H., III; Singh, D. L.; Kim, D.; Birge, R. R.; Bocian, D. F.; Holten, D.; Lindsey, J. S. *J. Am. Chem. Soc.* **1998**, *120*, 10001−10017. (g) Nakano, A.; Osuka, A.; Yamazaki, I.; Yamazaki, T.; Nishimura, Y. *Angew. Chem., Int. Ed. Engl.* **1998**, *37*, 3023−3027.

(7) (a) Denti, G.; Campagna, S.; Serroni, S.; Ciano, M.; Balzani, V. *J. Am. Chem. Soc.* **1992**, *114*, 2944−2950. (b) Belser, P.; von Zelewsky, A.; Frank, M.; Seel, C.; Vögtle, F.; De Cola, L.; Barigelletti, F.; Balzani, V. *J. Am. Chem. Soc.* **1993**, *115*, 4076−4086.

(8) (a) Ng, D.; Guillet, J. E. *Macromolecules* **1982**, *15*, 724−727. (b) Ng, D.; Guillet, J. E. *Macromolecules* **1982**, *15*, 728−732. (c) Guillet, J. E. *Polymer Photophysics and Photochemistry*; Cambridge University Press: Cambridge, 1985; pp 220−260. **(**d) Fox, M. A. *Acc. Chem. Res.* **1992**, *25*, 569−574. (e) Watkins, D. M.; Fox, M. A. *J. Am. Chem. Soc.* **1994**, *116*, 6441−6442. (f) Webber, S. E. *Chem. Rev.* **1990**, *90*, 1469−1482. (g) Jones, G., II; Rahman, M. A. *Chem. Phys. Lett.* **1992**, *200*, 241−250.

(9) (a) Xu, Z.; Moore, J. S. *Acta Polym.* **1994**, *45*, 83−87. (b) Devadoss, C.; Bharati, P.; Moore, J. S. *J. Am. Chem. Soc.* **1996**, *118*, 9635−9644. (c) Wang, P.-W.; Liu, Y.-J.; Devadoss, C.; Bharathi, P.; Moore, J. S. *Adv. Mater.* **1996**, *3*, 237−241. (d) Shortreed, M. R.; Swallen, S. F.; Shi, Z.-Y.; Tan, W.; Xu, Z.; Devadoss, C.; Moore, J. S.; Kopelman, R. *J. Phys. Chem. B* **1997**, *101*, 6318−6322. (e) Balzani, V.; Campagna, S.; Denti, G.; Juris, A.; Serroni, S.; Venturi, M. *Acc. Chem. Res.* **1998**, *31*, 26−34. (f) Jiang, D.-L.; Aida, T. *Nature* **1997**, *388*, 454−456. (g) Aida, T.; Jiang, D.-L.; Yashima, E.; Okamoto, Y. *Thin Solid Films* **1998**, *331*, 254−258. (h) Aida, T.; Jiang, D.-L. *J. Am. Chem. Soc.* **1998**, *120*, 10895−10901. (i) Kawa, M.; Fréchet, J. M. J. *Chem. Mater.* **1998**, *10*, 286−296.

10.1021/ja993272e CCC: $19.00
Published on Web 01/29/2000

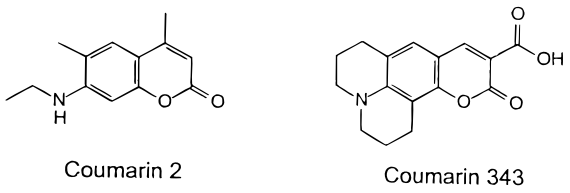

Figure 1. Structures of the donor and acceptor dyes used for dendrimer functionalization.

teractions leading to energy transfer were difficult to control since linear polymers fold into random coils with shapes that vary with solvent, temperature, and pH. More recently, detailed investigations into multiporphyrin assemblies as model systems for light harvesting and energy transfer have been described.[6a−f] Energy transfer from Zn porphyrins to free base (Fb) porphyrins can occur within these assemblies with efficiencies in excess of 90%. The covalent nature of the porphyrin linking units enables precise control over the architecture of these multiporphyrin arrays. Indeed, complex structures in which a central Fb porphyrin is surrounded by four Zn porphyrins have been prepared and studied.[6b−d] Such assemblies begin to resemble the natural photosynthetic units in which a large number of donor chromophores surround a single acceptor unit (the reaction center). However, it has been demonstrated that within these assemblies, energy transfer occurs predominantly by a through-bond mechanism due to the conjugation that exists within the inter-porphyrin linkers.[6c] This through-bond mechanism severely limits the distance across which energy transfer is efficient, and hence it places structural limitations on the porphyrin assemblies themselves. An additional drawback of these systems is the relatively low quantum yield of fluorescence of the porphyrins, which could restrict their use in practical photonic devices such as light-emitting diodes, fluorescent sensors, frequency converters, and signal amplifiers.

The use of dendrimers[10] for light harvesting has been elegantly demonstrated by several groups.[9] Most notably, Moore and co-workers developed a system based on phenyl acetylene dendrimers and showed an energy cascade from the dendrimer to a lone perylene chromophore at the focal point. In this system, energy transfer is extremely efficient, even at high generations. However, due to the cross-conjugated nature of the dendrimer framework, it is difficult to determine whether the energy-transfer mechanism was through bond or through space. Using a different system based on poly(aryl ether) dendrimers, Aida and co-workers have shown that multiple low-energy photons could be harvested by the dendrimer and transferred to an azobenzene core, accelerating its isomerization from *cis*- to *trans*-azobenzene.[9f,g] Previous work from our group has also shown that a poly(aryl ether) dendritic shell surrounding lanthanide ions can amplify the emission of the core through an antenna effect.[9i]

More recently, we have reported preliminary results on the synthesis and characterization of a novel family of laser-dye functionalized "reversed" poly(aryl ether) dendrimers.[11] In these molecules, a number of coumarin 2 dyes (Figure 1) are placed at the peripheral chain ends of the dendrimer and a single coumarin 343 is placed at the core. It has been found that, upon excitation of the peripheral coumarin 2 dyes, the absorbed energy is quickly and efficiently transferred to the focal coumarin 343. It has previously been shown that the electronic absorption spectrum of the dendritic backbone lies entirely below 300 nm,[9h] well separated from the absorption and fluorescence bands of the coumarins. Hence, the role of the dendritic backbone is a structural rather than functional one: the dendrimer acts as a scaffold that holds the two types of interacting laser-dyes in a desired spatial arrangement and does not play a role in energy transfer. Thus, the dendritic scaffold may be chosen to fulfill other requirements such as specific reactivity, ease of processability, capacity for encapsulating guest molecules, etc. Also, the dyes may be varied to provide additional features such as wavelength tunability, enhanced solubility, and reactivity. This report describes the detailed photophysical properties and energy-transfer efficiencies of the synthesized dendrimers. Steady-state absorption and fluorescence data in several solvents, as well as time-resolved fluorescence data, are also presented.

Results and Discussion

Purity, Solubility, and Stability of the Dendrimers. The synthesis of generation 1 (G-1) to generation 4 (G-4) coumarin-labeled dendrimers (Figure 2) along with all relevant model compounds (Figure 3) has previously been described.[11] To conduct reliable spectroscopic analysis of the dendrimers, their purity, solubility, and stability must be ascertained. The dendrimers were purified by chromatography on silica gel and fully characterized by ^{1}H and ^{13}C NMR, elemental analysis, high-performance liquid chromatography (HPLC), and Matrix-assisted laser desorption/ionization (MALDI-TOF) mass spectrometry. The purity of the dendrimers, as determined by HPLC, was found to be in excess of 95% (Figure 4). Interestingly, the only impurities found in the samples were molecules having lost a single peripheral coumarin 2 dye that could not be separated from the fully labeled dendrimers by column chromatography. The identification of these impurities was based on MALDI-TOF data, which show a peak corresponding to the loss of 200 mass units, consistent with the replacement of a coumarin with a hydroxyl group. Additionally, the UV/visible absorption spectrum of the impurity (measured with a diode array HPLC detector) clearly shows the presence of both donor and acceptor absorptions (vide infra), with the donor absorption being attenuated to the degree expected for the loss of one coumarin 2 (i.e., approximately decreased by 1/2 in G-1, 1/4 in G-2, etc.) Due to the similarity of this impurity to the desired compound, its presence is not expected to significantly affect the photophysical measurements performed with the dendrimer series **1**−**4**. The dendrimers were soluble in a variety of organic solvents such as CH_2Cl_2, $CHCl_3$, THF, and toluene. Somewhat lower solubility in acetonitrile was observed for **1**−**3**, and **4** was found insoluble in this solvent. In methanol, solubility was limited only to the first two generations. Finally, the molecules were stable during normal manipulation, and no special handling was necessary.

Steady-State Absorption Properties. The absorption spectra of the dendrimer series **1**−**4**, along with model compounds **5**−**9**, were measured in toluene, acetonitrile (except for **4**), and methanol (**1** and **2** only). The wavelengths of maximum absorption (λ_{max}) and molar extinction coefficients (ϵ) are collected in Table 1. Figure 5 illustrates the absorption spectra of the dendrimer series in toluene. From these spectra, two

(10) (a) Tomalia, D. A.; Naylor, A. M.; Goddard, W. A., III *Angew. Chem., Int. Ed. Engl.* **1990**, *29*, 138−175. (b) Fréchet, J. M. J. *Science* **1994**, *263*, 1710−1715. (c) Fréchet, J. M. J.; Hawker, C. J. In *Synthesis and Properties of Dendrimers and Hyperbranched Polymers, Comprehensive Polym. Sci.*, 2nd Suppl.; Aggarwal, S. L., Russo, S., Eds.; Pergamon Press: Oxford, 1996; p 140. (d) Newkome, G. R.; Moorefield, C. N.; Vogtle, F. *Dendritic Molecules: Concepts, Syntheses, Perspectives*; VCH: Weinheim, 1996.

(11) (a) Gilat, S. L.; Adronov, A.; Fréchet, J. M. J. *Angew. Chem., Int. Ed.* **1999**, *38*, 1422−1427. (b) Gilat, S. L.; Adronov, A.; Fréchet, J. M. J. *J. Org. Chem.* **1999**, *64*, 7474−7484.

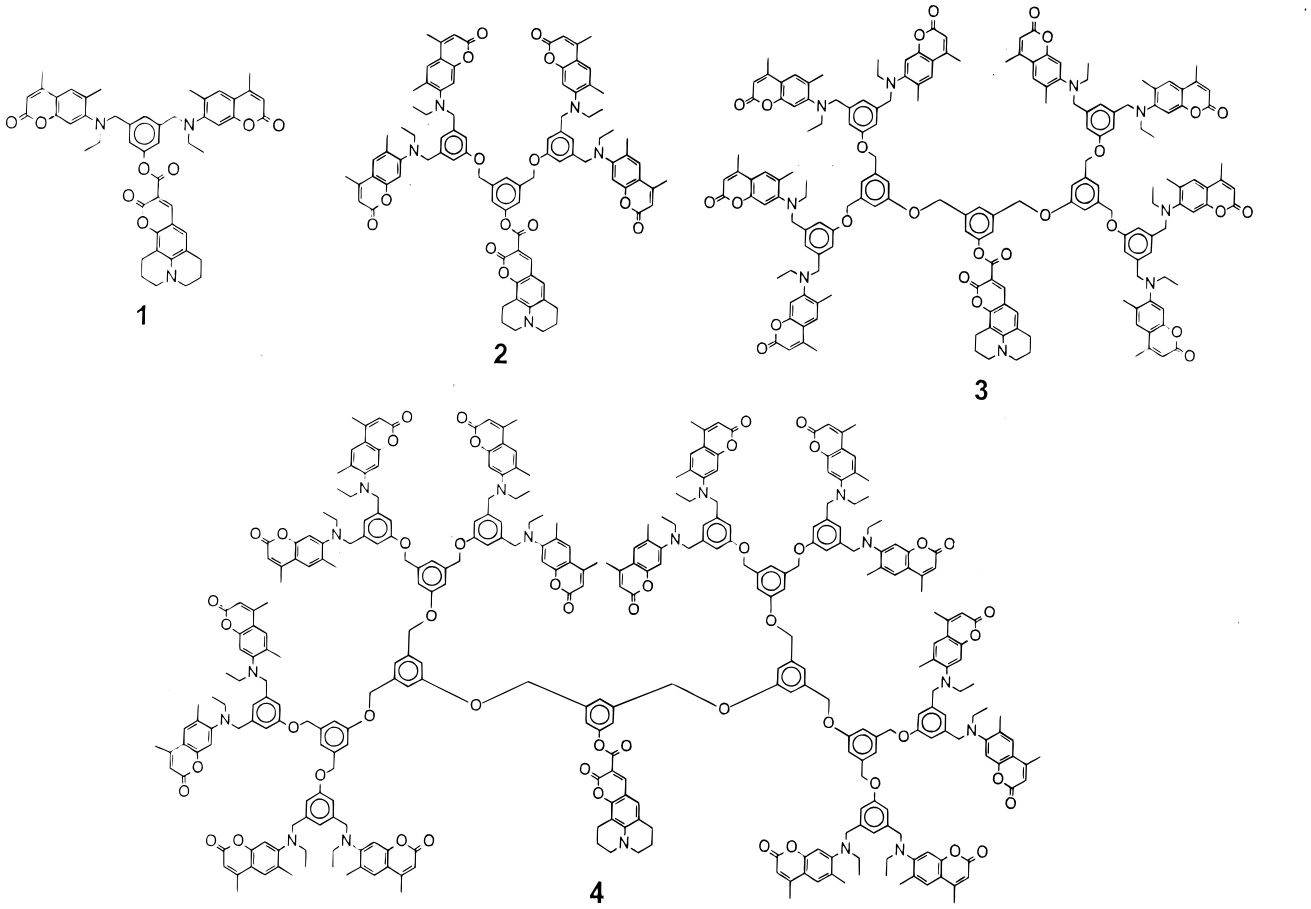

Figure 2. Structures of the G-1−G-4 donor and acceptor labeled dendrimer series.

separate absorption bands that correspond to the individual absorptions of the coumarin 2 donors (310−380 nm) and the coumarin 343 acceptor (400−480 nm) can be discerned. As the dendrimer generation increases, so does the absorption due to the peripheral chromophores, which, as expected, doubles from one generation to the next, within experimental error. Hence, with increasing generation, the amount of light that the peripheral antenna is capable of harvesting is dramatically enhanced. It should also be noted that there is no spectral broadening or spectral shift of the donor absorption band with increasing generation (λ_{max} = 343−344 nm for the entire dendrimer series). The absorption intensity of the lone focal acceptor dye does not significantly change with increasing generation but does exhibit a 6 nm bathochromic shift (in toluene) which is attributed to solvatochromic behavior. It has previously been demonstrated that the polarity of the environment of the core increases with increasing dendrimer size.[12] Bathochromic shifts in coumarin absorptions with increased medium polarity are also well documented.[13] Hence, in our case, it may be stated that increasing dendrimer size increases the polarity of the environment of the core (relative to toluene) and that this phenomenon is responsible for the shift in acceptor λ_{max}. When the solvent was changed to CH_3CN or MeOH, the ϵ values of the dyes were observed to increase slightly for all of the molecules (Table 1). However, in these polar solvents, the bathochromic shift of the acceptor as a function of increasing dendrimer generation was much less pronounced, since the increased polarity of the larger dendrimer backbone is no longer significant in comparison to the polarity of the solvent that surrounds the core dye of the molecules.

The ground-state behavior of the fully dye-functionalized dendrimers can be studied through comparison with model compounds **5** and **9** (Figure 3). The absorption spectra of **5** and **9**, as well as that of a G-1 dendron (**1**) are shown in Figure 6. The absorption spectrum of the dendron in the 300−500 nm region closely matches the sum of the absorptions of the two model compounds. This indicates that, within the dendritic structure, the individual dyes do not exhibit any specific interactions in the ground state and confirms that the dendrimer backbone is transparent in this λ range. Additionally, it should be noted that the absorption spectrum of the acceptor dye is significantly red-shifted from that of the donors. Such complementary absorptions provide greater spectral coverage (>150 nm) and enhancement of the overall light-harvesting capabilities of these dendrimers.

It was observed that the ϵ value per donor dye (coumarin 2) of the dendrons was significantly diminished when compared to that of the nonalkylated dye (Table 1). This difference can be rationalized by the fact that alkylation of the nitrogen of coumarin 2 decreases the alignment of its lone pair orbital with the aromatic system of the dye due to steric hindrance that forces a deviation from coplanarity. This, in turn, decreases conjugation with the aromatic coumarin and affects the ϵ value. Using molecular modeling (Molecular Simulations Inc. Insight II software), it was verified that the minimized structure of an alkylated coumarin 2 molecule indeed exhibits a twisting of the N lone pair orbital away from coplanarity. Additionally, the monofunctionalized first-generation analogue **10** (Figure 3),

(12) Hawker, C. J.; Wooley, K. L.; Fréchet, J. M. J. *J. Am. Chem. Soc.* **1993**, *115*, 4375−4376.

(13) (a) Arbeloa, T. L.; Arbeloa, F. L.; Tapia, M. J.; Arbeloa, I. L. *J. Phys. Chem.* **1993**, *97*, 4704−4707. (b) Jones, G., II; Jackson, W. R.; Choi, C.; Bergmark, W. R. *J. Phys. Chem.* **1985**, *89*, 9, 294−300.

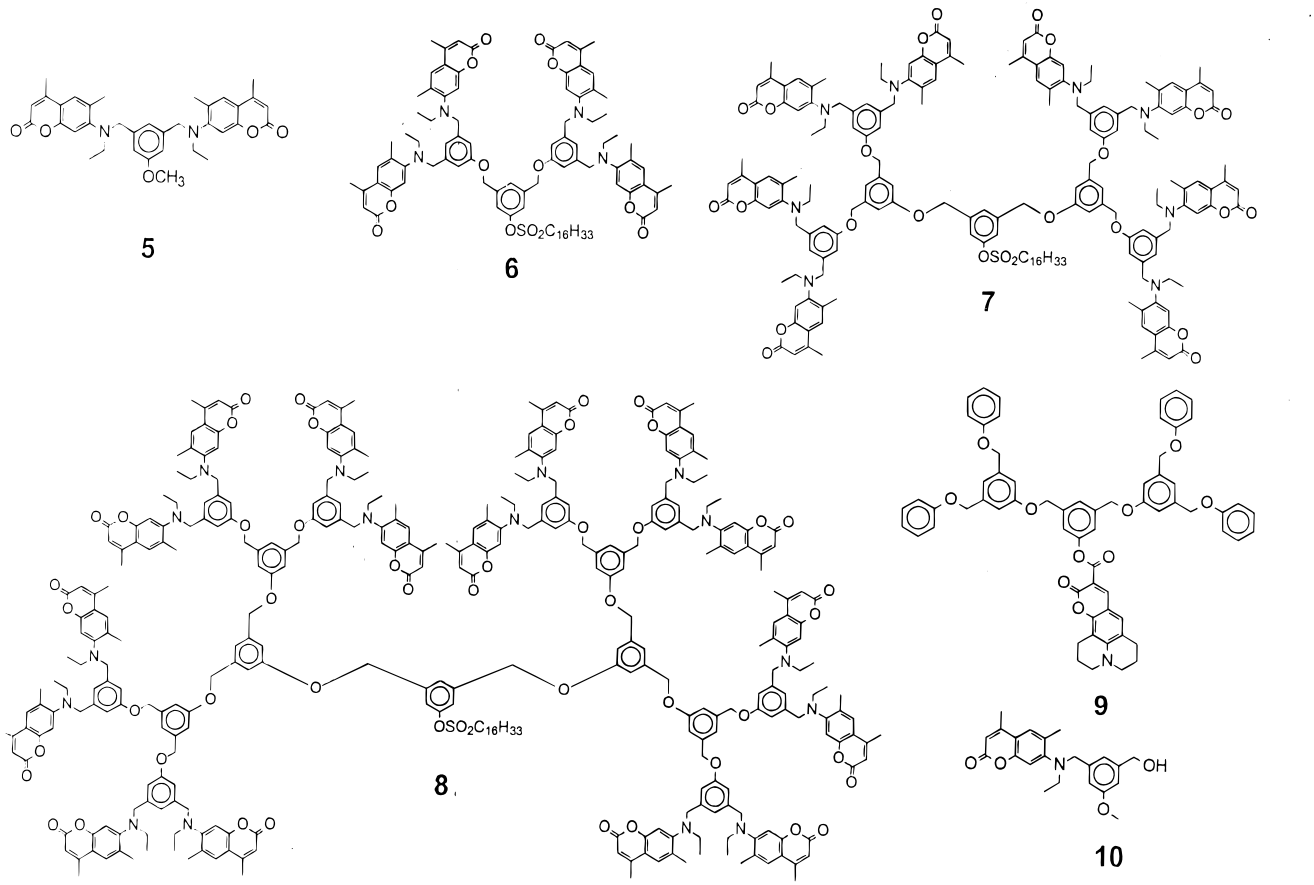

Figure 3. Structures of the donor model compounds (**5**−**8**), acceptor model compound (**9**), and monofunctionalized G-1 analogue (**10**).

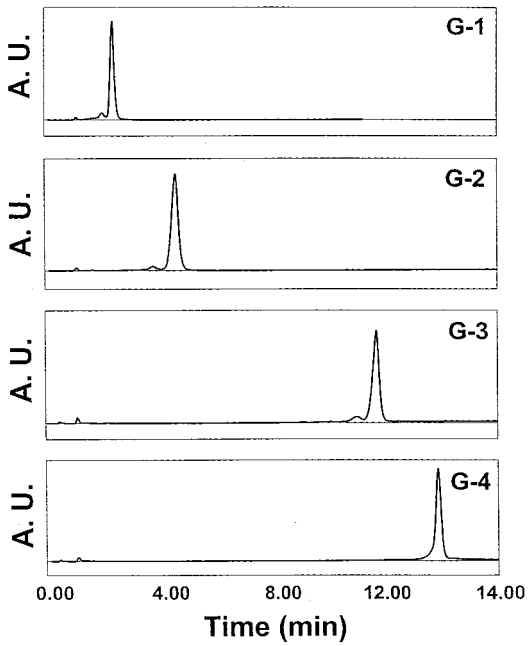

Figure 4. HPLC traces for the fully dye-labeled dendrimers **1**−**4**.

which was a byproduct of the G-1 synthesis, was found to have an ϵ of ~13 000 cm^{-1} M^{-1}. This value is significantly lower than the ϵ of coumarin 2 (20 000) and matches well with half of the value for the first-generation dendrons containing two donors (ϵ = 25 000). Hence, the drop in ϵ is due to alkylation of the N rather than an interaction with another nearby coumarin. Although the donor ϵ decreases significantly upon alkylation, its value is still rather high and does not preclude the synthesis of strongly absorbing dendrimers.

Table 1. Values of λ_{max} and ϵ for the Dendrimers and Model Compounds in Toluene, CH_3CN, and CH_3OH

	λ_{max}, nm (ϵ, M^{-1} cm^{-1})		
compd	toluene	CH_3CN	CH_3OH
1	343 (25 000)	343 (26 000)	346 (27 000)
	437 (46 000)	442 (49 000)	445 (52 000)
2	344 (49 600)	344 (52 400)	346 (49 500)
	438 (45 500)	442 (50 700)	446 (49 300)
3	344 (88 500)	344 (98 000)	
	441 (36 000)	446 (42 700)	
4	344 (152 000)		
	443 (38 000)		
5	343 (25 500)	344 (27 600)	347 (27 900)
6	343 (50 000)	344 (54 700)	348 (54 600)
7	343 (94 000)	343 (102 000)	
8	343 (184 000)		
9	437 (42 500)	442 (49 000)	444 (37 000)
Coumarin 2	349 (20 300)	356 (21 000)	366 (21 000)
Coumarin 343	440 (41 000)	448 (42 000)	444 (39 700)

Steady-State Fluorescence. A comparison of the absorption and emission spectra of the model donor and acceptor compounds is presented in Figure 7. From this figure, it can be seen that the overlap of the donor emission and the acceptor absorption is extremely large (gray area), especially when compared to the overlap of the donor emission with its own absorption (black area). The large spectral overlap between the two interacting chromophores indicates that the probability of donor−acceptor energy transfer should be high (vide infra). The fluorescence emission spectra of the dendrimer series **1**−**4** in toluene (4.09×10^{-6} M) are shown in Figure 8. Data reporting the wavelengths of maximum emission intensity (λ_{em}) and fluorescence quantum yields (Φ_F) for this series and all model compounds in toluene, acetonitrile, and methanol are listed in

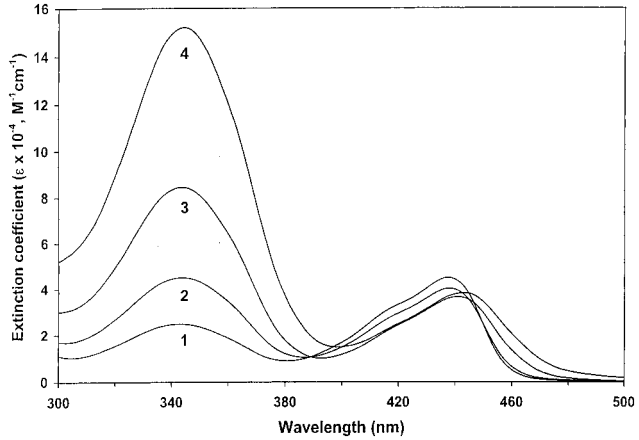

Figure 5. Absorption spectra for the dendrimer series **1**−**4** in toluene.

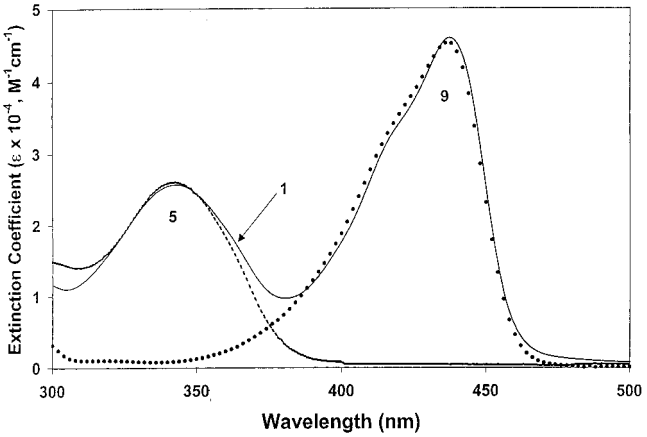

Figure 6. Absorption spectra of the G-1 donor model compound **5** (dashed), acceptor model compound **9** (dotted), and the fully dye-labeled dendron **1**.

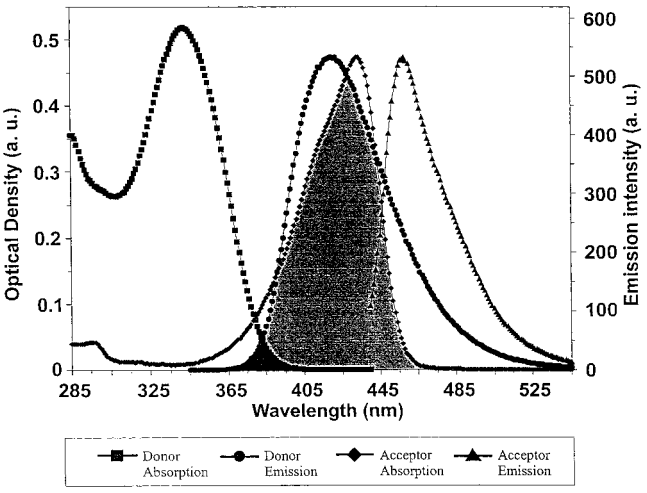

Figure 7. Absorption and emission spectra of the model donor (**6**) and acceptor (**9**) compounds with the donor−acceptor spectral overlap indicated in gray and donor−donor spectral overlap indicated in black.

Table 2. Excitation of the dendrimer series **1**−**4** at 343 nm (the donor absorption maximum) resulted in emission emanating predominantly from the acceptor dye at ∼480 nm. The almost complete disappearance of donor emission at 420 nm, along with the strong acceptor emission, indicates that energy-transfer efficiency is extremely high in these molecules. The dotted line in Figure 8 illustrates the direct core emission of the third-generation dendrimer when excited at 441 nm (where the peripheral donor dyes do not absorb) after correction for the lamp output difference at this wavelength. A comparison of the intensity of this direct emission with the intensities from sensitized emission of the G-3 and G-4 dendrimers indicates that it is possible to gain a more intense emission from the core when it is excited via sensitization from a large light-harvesting antenna than when it is directly excited by photons at its absorption maximum.[14] This observation indicates not only that the large light-harvesting antenna is more efficient than the core dye at capturing photons from its environment but also that the energy-transfer interaction is extremely efficient.

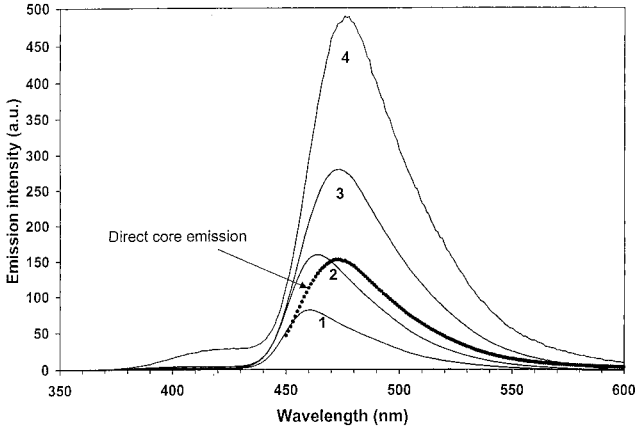

Figure 8. Emission spectra of the dendrimer series **1**−**4** in toluene along with the direct core emission (λ_{ex} = 441 nm, dotted).

Table 2. Values of λ_{em} and Φ_F for the Dendrimers and Model Compounds in Toluene, CH_3CN, and CH_3OH

	λ_{em},[a] nm (Φ_F)		
compd	toluene	CH_3CN	CH_3OH
1	461 (0.67) (0.54)	483 (0.81) (0.65)	486 (0.86) (0.71)
2	464 (0.60) (0.54)	482 (0.75) (0.69)	484 (0.53) (0.50)
3	473 (0.51) (0.54)	484 (0.50) (0.50)	
4	475 (0.38) (0.38)		
5	417 (0.66)	457 (0.20)	445 (0.010)
6	419 (0.54)	458 (0.23)	448 (0.014)
7	424 (0.50)	452 (0.22)	
8	427 (0.40)		
9	461 (0.54)	482 (0.77)	484 (0.80)
coumarin 2	403 (0.64)	423 (0.98)	440 (0.97)
coumarin 343	463 (0.58)	488 (0.81)	487 (0.84)

[a] The second value in parentheses indicates the Φ_F for the acceptor when directly excited.

The emission spectra of the donor and acceptor model compounds in toluene (2.14×10^{-6} M) are illustrated in Figure 9. As expected, excitation of the peripheral chromophores in each generation of donor model compounds at 343 nm resulted in fluorescence at ∼420 nm. Excitation of the acceptor model compound **9** with the same light intensity at 343 nm resulted in almost no emission, as seen from curve 9b (Figure 9). This illustrates the fact that the two types of chromophores in the dendritic structure can be separately addressed by varying the illumination wavelength, since their absorption spectra do not overlap appreciably. Excitation of **9** at 441 nm resulted in its own emission centered at ∼470 nm (curve 9a, Figure 9).

(14) The direct core emission was measured by exciting the G-3 dendrimer sample used to obtain curve 3 (Figure 8) at 441 nm, which was then corrected for the lamp intensity difference (relative to 343 nm lamp output) and concentration. When normalized for concentration, the intensity of the direct core emission remained constant for all dendrimer generations studied.

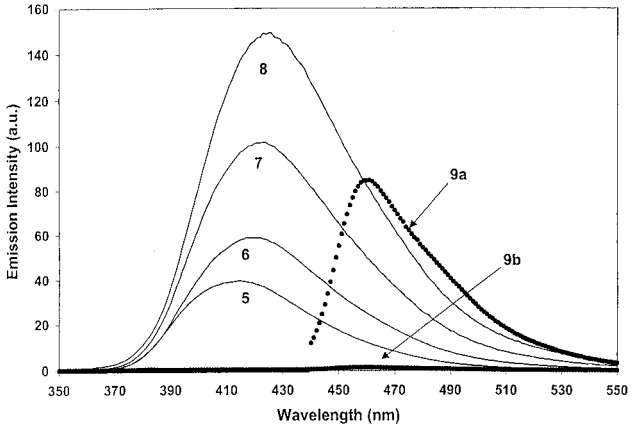

Figure 9. Emission spectra of the model donor series **5**−**8** ($\lambda_{ex} = 343$ nm) and the model acceptor **9** (a, $\lambda_{ex} = 441$ nm; b, $\lambda_{ex} = 343$ nm) in toluene, normalized to a concentration of 2.143×10^{-6} M.

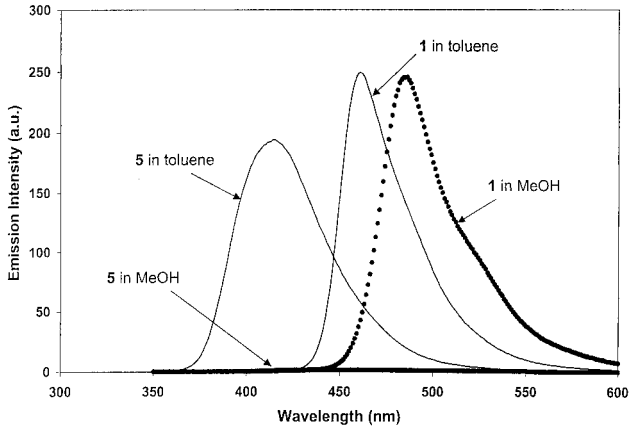

Figure 10. Comparison of emission spectra of the first-generation dendrimer **1** and model donor compound **5** in toluene (solid) and MeOH (dotted).

Figure 5 shows that the amount of light absorbed by the peripheral dendritic antenna doubles from one generation to the next. Hence, it would be reasonable to expect that the emission intensity of the donor dyes in the absence of acceptor should also double. However, the spectra in Figure 9 clearly show that this is not the case. This less than 2-fold increase in emission intensity from the donor model compounds indicates that as the dendrimer generation increases, the number of nonradiative relaxation pathways, along with their rate, must also increase.[9b] Hence these nonradiative pathways begin to effectively compete with the rate of fluorescence, thereby decreasing the Φ_F of the donor chromophores (Table 2). The possibility of this quenching being due to reabsorption of emitted photons was ruled out by performing dilution experiments and by comparing the results obtained from right-angle and front-face fluorescence measurements. All dilution experiments resulted in decreased emission intensities that were proportional to the dilution factor, and front-face experiments yielded spectra that gave identical results to right-angle emission studies. Interestingly, at constant concentration, the doubling of emission intensity with dendrimer generation *is restored* in the presence of the acceptor dye (Figure 8). In this case, although the wavelength range of the emission is now characteristic of the acceptor, the increase in emission intensity correlates well with the donor absorption increase from one generation to the next (Figure 5). These observations indicate that the energy-transfer process in the dendrimers occurs on a faster time scale than any other radiative or nonradiative event originating from the donors, even at high generations.

The fluorescence behavior of the dendrimer series **1**−**4**, along with the model compounds, in different solvents (toluene, CH_3CN, MeOH) also shows interesting trends. Unfortunately, as the dendrimer generation increases, the molecules become less soluble in the more polar solvents and some measurements could not be performed. It can be seen, however, that upon changing the solvent from toluene to either CH_3CN or MeOH, λ_{em} is red-shifted much more dramatically than λ_{max}. This bathochromic shift is expected since a more polar solvent is able to stabilize the charge-separated excited state of the coumarin dyes. Again, as the dendrimer generation increases, a bathochromic shift is observed for core emission in toluene solution, but an analogous shift is not observed in CH_3CN or MeOH. The shifts in the fluorescence spectra may be explained using the same reasoning as for the shifts in absorption spectra (vide supra). Interestingly, it was found that the quantum yields of fluorescence for the donor model compounds **5**−**8** drop dramatically when the solvent is changed from toluene to either CH_3CN or MeOH. In fact, almost complete quenching of emission in MeOH is observed for **5** and **6** (Table 2). This behavior has been observed previously for alkylated 7-aminocoumarin dyes[13] and is not specifically caused by the presence of the dendrimer backbone. However, it is important to note that quenching of the acceptor model compound **5** does not occur in methanol, and the Φ_F values of the fully dye-labeled dendrimers remain high in the more polar solvents. This is illustrated graphically in Figure 10, which compares the emission spectra of the G-1 dendrimer with (**1**) and without (**5**) the acceptor chromophore as the solvent is changed from toluene to MeOH. In the presence of the acceptor, the energy that would otherwise be lost is salvaged and converted into a strong emission. Indeed, emission of the fully labeled molecule is nearly as intense in MeOH as it is in toluene (Figure 10). The observation that efficient energy transfer still occurs in MeOH again indicates that energy transfer occurs much faster than any deactivating process responsible for quenching the donor chromophores in this solvent. The observed lack of environmental sensitivity of the energy-transfer interaction in these molecules may be important to the eventual utility of similar systems in the fabrication of commercial photonic devices.

Time-Resolved Measurements. To further investigate the rates of energy transfer in these molecules, time-resolved fluorescence measurements were undertaken. Fluorescence decays for both the model compounds and the fully dye-labeled dendrimers were carried out in toluene and acetonitrile solution using the time-correlated single-photon-counting method. The samples were excited at 340 nm, and the fluorescence decay was monitored at the emission maximums: 420 nm for the donor model compounds and 470 (in toluene) or 480 nm (in CH_3CN) for the fully dye-labeled dendrimers. In the fully labeled dendrimers, emission at 420 nm was also monitored to determine whether a residual decay from the donor dyes could be detected. A typical fluorescence decay trace is given in Figure 11 and the entire set of acquired data is summarized in Table 3.

Contrary to the data reported for phenylacetylene dendrimers by Moore and co-workers,[9b] almost none of the structures we investigated exhibit monoexponential decay profiles (the only exceptions being model compounds **5** and **6** when measured in acetonitrile). To rule out the possibility of the involvement of impurities in this non-monoexponential behavior, extensive repurification was carried out with no change in the results. The acquired data were arbitrarily fitted with multiexponential equations, using the minimum number of exponentials needed

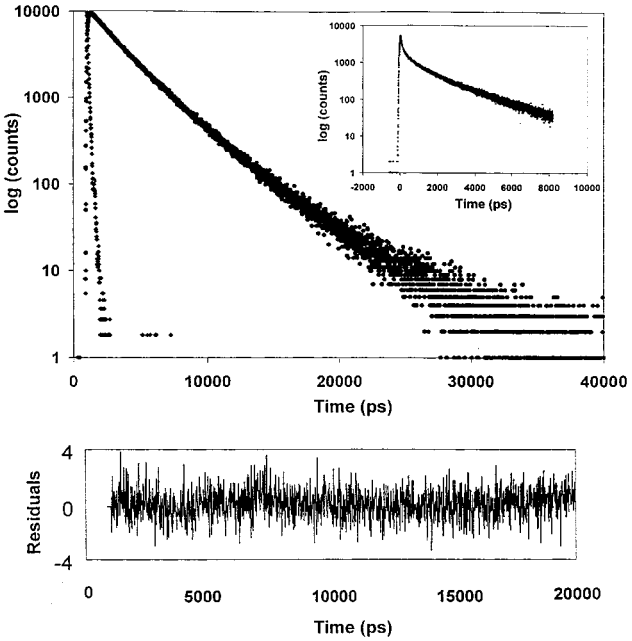

Figure 11. Fluorescence decay trace for the G-4 dendrimer **4** in toluene with the excitation $\lambda = 340$ nm and the detection $\lambda = 470$ nm. The instrument response function (◆) and the fluorescence decay trace (●) are shown. The decay profile was fitted to a triexponential function, producing the indicated residuals and a χ^2 value of 1.08. Inset shows the quenched donor emission in the presence of the acceptor for the G-4 dendrimer detected at 420 nm (the long-lived decay is due to the fluorescence tail of the core).

Table 3. Fluorescence Lifetimes for Dendrimers **1**−**4** in Toluene Measured at 470 nm, **1**−**3** in Acetonitrile Measured at 480 nm, **5**−**8** in Toluene Measured at 420 nm, and **5**−**7** in Acetonitrile Measured at 420 nm

compd	τ_1 (ps)	a_1[a]	τ_2 (ps)	a_2	τ_3 (ps)	a_3	τ_{av} (ps)
			Section a				
1	90	−0.24	1542	0.16	2404	0.84	2266
2	67	−0.22	1834	0.33	2717	0.67	2422
3	36	−0.51	1885	0.68	3645	0.32	2455
4	59	−0.54	2052	0.68	3896	0.33	2636
			Section b				
1	6.4	−0.9			2955	1	
2	13.1	−0.55			2706	1	
3	50	−0.27	1570	0.51	3002	0.49	2270
			Section c				
5			954	0.08	2831	0.92	2673
6			1255	0.35	3047	0.65	2409
7	393	0.20	1671	0.46	3324	0.34	1979
8	339	0.25	1690	0.44	3683	0.31	1964
			Section d				
5	62.9	0.30	1257	0.16	3804	0.54	2268
6	138	0.32	1647	0.22	4253	0.46	2372
7	223.4	0.26	2043	0.32	4728	0.42	2700

[a] Negative amplitudes indicate rise components.

to give an acceptable χ^2 value. This treatment produced fitted decays that matched the observed data extremely well in most cases. However, it should be noted that the number of exponentials used is merely a qualitative indication of the degree of inhomogeneity in the system and is not intended to signify the exact number of distinct processes being observed. The explanation we propose for the non-monoexponential behavior involves the flexible nature of the dendrimers, especially when compared to their phenylacetylene counterparts.[9a−d] As a result of the conformational freedom of the dendritic backbone, significant motion and even folding of branches can occur, thereby creating a variety of local microenvironments for the individual dyes. Since the photophysical properties of coumarins are known to be extremely sensitive to environmental parameters such as solvent polarity,[13] it is likely that small changes in the local microenvironment (i.e., dendrimer conformations) will alter the fluorescence lifetimes of the individual dyes. Such a phenomenon would be expected to become even more significant at higher generations due to their greater conformational freedom, and this is observed in the relative amplitudes of the different components in the fluorescence decays (Table 3). Additionally, in the model donor compounds of higher generation (G-3, G-4), we observed some fast decay components on the order of several hundred picoseconds. These fast decays are ascribed to local concentration quenching[15] since, as the size, flexibility, and number of donor dyes in the dendrimer increases, the probability of having two dyes close enough to promote this type of nonradiative quenching will also increase. This phenomenon is not observed with the fully labeled dendrimers since a high local concentration of the core dye does not exist in these systems. It must be emphasized here that the dendrimers used in this study are too small to be affected by the "De Gennes dense packing"[16] that would lead to restricted motion of the peripheral functionalities as observed by Tomalia with his largest PAMAM dendrimers[17] or by Meijer in his "dendritic box".[18]

The generation-dependent trends in the time-resolved data show that, for the fully labeled dendrimers **1**−**4**, the average lifetime in toluene increases from 2.27 ns for **1** to 2.64 ns for **4**, while in acetonitrile, the lifetime decreases from 2.96 ns for **1** to 2.27 ns for **3**. To rationalize these observations, it is important to note that previous photophysical studies of coumarin laser-dyes indicate that their fluorescence lifetime lengthens with increasing solvent polarity.[13b] Hence, an argument similar to that presented for the bathochromic shifts in the steady-state core emission spectra (vide supra) can again be utilized. In toluene, the acceptor is exposed to a less polar environment at low generation than at high generation, so its fluorescence lifetime should increase with generation. In contrast, when acetonitrile is the solvent, the core is exposed to a more polar environment at low generation than at high generation, which accounts for the decrease in fluorescence lifetime. Interestingly, the average lifetime of the core emission of the G-3 dendrimer is very similar in both toluene and acetonitrile (2.45 and 2.27 ns, respectively).

For the donor model compounds **5**−**8**, the trend of the fluorescence lifetimes is exactly reversed. In toluene, the average fluorescence lifetime decreases from 2.67 to 1.96 ns for the series, while in acetonitrile the lifetime increases from 2.27 ns in **5** to 2.70 ns in **7**. Again, as the dendrimer generation increases, it is reasonable to assume that the number of nonradiative relaxation pathways for the peripheral chromophores should increase, thereby decreasing their fluorescence lifetime.[9b] The trend in toluene is consistent with this assumption. The exact reason for the inconsistency in the acetonitrile data for the donors is currently under investigation.

Attempts to measure the lifetime of the quenched donor fluorescence in the presence of the acceptor, as well as the rise time of sensitized acceptor fluorescence (**1**−**4**), were only

(15) (a) Bojarski, P. *Chem. Phys. Lett.* **1997**, *278*, 225−232. (b) Indig, G. L.; Wilson, T. *J. Photochem. Photobiol. A: Chem.* **1992**, *63*, 195−199. (c) Guilford, J., II; Bergmark, W. R. *J. Photochem.* **1984**, *26*, 179−184.
(16) De Gennes, P. G.; Hervet, H. *J. Phys. Lett.* **1983**, *44*, L-351−L-360.
(17) Tomalia, D. A.; Durst, H. D. *Top. Curr. Chem.* **1993**, *165*, 193−313.
(18) Jansen, J. F. G. A.; de Brabander-van den Berg, E. M. M.; Meijer, E. W. *Science* **1994**, *266*, 1226−1229.

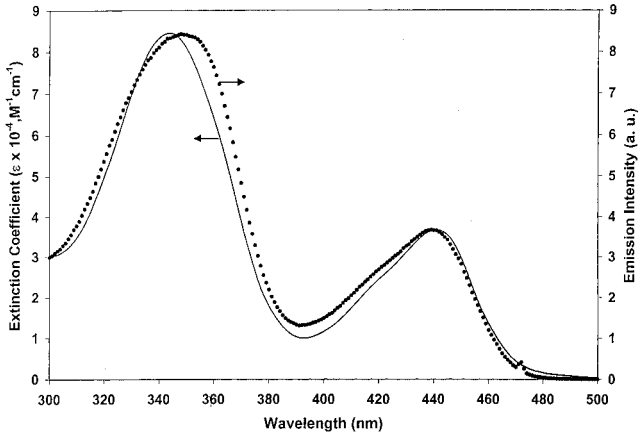

Figure 12. Comparison of absorption (solid) and excitation (dotted) spectra of the G-3 dendrimer **3**.

partially successful. The quenched donor decays could not be measured for the first three generations since the signal at 420 nm was much weaker than the fluorescence tail of the acceptor dye at the same wavelength. However, in the fourth generation, a 59 ps decay component was detected at 420 nm (Figure 11, inset), which is consistent with the rise time of core fluorescence (Table 3, parts a and b). Although all of the rise components of the core could not be accurately resolved for the entire dendrimer series, it is possible to place an upper limit of 30 ps[19] for the average rise time for G-1 to G-3 and of 40−50 ps for G-4.

Energy-Transfer Calculations. The singlet−singlet excitation energy-transfer efficiencies from the peripheral coumarin 2 donors to the core coumarin 343 acceptor can be estimated using steady-state and time-resolved fluorescence data. Initially, we sought to obtain the transfer efficiency through comparison of the absorption and fluorescence excitation spectra of the fully dye-labeled dendrimers, and the result for G-3 is shown in Figure 12. The similarity between the absorption and excitation spectra qualitatively attests to the nearly quantitative energy transfer for this molecule. However, precise calculations using this method proved troublesome. Since this approach relies on a direct comparison of data acquired from two different instruments, requires accurate correction of the excitation spectrum, and assumes that the acceptor quantum yield remains constant upon both direct and sensitized excitation, significant errors can be introduced. Indeed, our primary calculations suggested energy-transfer efficiencies greater than 100% for the first three generations, which are clearly erroneous. Hence we determined the energy-transfer efficiency by studying the quenching of the donor fluorescence in the presence of the acceptor, a method that is less prone to error.[20] The availability of exact donor model compounds (**5**−**8**) gave easy access to the unquenched donor emission spectra, which are required for the calculation. This method revealed that, in toluene, the donor emission was quenched over 40-fold in the first three generations, indicating an energy-transfer efficiency of greater than 97% (Table 4). This quenching was less effective in the fourth generation, and the energy-transfer efficiency was originally calculated to be 86%.[11a] Similar results were obtained using CH_3CN as the solvent. However, it is important to point out that the accuracy of steady-state measurements is lower when energy-transfer efficiencies are nearly quantitative and the measurements are extremely susceptible to errors resulting from the presence of trace impurities. In such highly efficient systems, it is necessary to confirm the steady-state measurements with time-resolved fluorescence data. Although it was not possible to detect quenched donor decays in all but the fourth generation (vide supra), an upper limit to the rise time of the core emission could be assigned. The magnitude of this rise time corresponds to the rate of energy transfer and can be used to determine the energy-transfer efficiency (Table 4). As can be seen from the calculated values, a nonnegligible discrepancy exists between the energy-transfer efficiencies from steady state vs time-resolved data for **4**. The time-resolved data clearly suggest that our previous estimate (86%) was too low. Currently, our only explanation for this discrepancy is the possibility that some trace impurities consisting of dendrimers without the core dye were present in the samples used for steady-state analysis. These impurities would not affect the time-resolved measurements since their long-lived (unquenched) fluorescence decay can be separated from the decay of the quenched donors. Indeed, once this observation was made, a more rigorous purification of the G-4 sample yielded a steady-state spectrum with a decreased emission intensity at 420 nm, corresponding to a measured energy-transfer efficiency of ∼93% (Table 4). This value is now within experimental error (±5%) of the value measured by time-resolved methods.

Table 4. Estimated Energy-Transfer Efficiencies for Compounds **1**−**4** from Both Steady-State and Time-Resolved Data

	energy-transfer efficiency (%)		
	steady state		time resolved
compd	toluene	acetonitrile	toluene/CH_3CN
1	98.1	92.0	98.9[b]
2	97.2	97.2	98.8[b]
3	97.5	94.5	98.5[b]
4	86.4 (92.7)[a]		97.5[c]

[a] Value in parentheses was obtained from a carefully repurified sample. [b] Values based on a 30 ps rise time. [c] Value based on a 50 ps rise time.

Mechanism of Energy Transfer. For energy-transfer processes involving allowed optical transitions, the Coulombic mechanism, which in its point−dipole approximation is referred to as the Förster mechanism,[21] is expected to dominate. Orbital overlap contributions to the electronic coupling may also be significant at very short donor−acceptor separations[22]—one such contribution arising from electron exchange is referred to as Dexter transfer.[23] In detailed studies of photosynthetic light-harvesting complexes, we have concluded that the Coulombic mechanism, when generalized to account for the full spatial distribution of the donor and acceptor transition densities (the transition density cube method),[24] can quantitatively describe the ultrafast energy-transfer rates. Given the large transition moments, high Φ_F values, high ϵ values, and good overlap between donor emission and acceptor absorption (Figure 7), the Coulombic mechanism is expected to dominate here also. However, because we currently lack detailed structural information, we utilize the theory in its simplest form—that of Förster

(19) Our instrument response function of the time-resolved fluorescence apparatus was typically 80 ps, which, after deconvolution, allows for the resolution of ∼30 ps events.

(20) Mugnier, J.; Pouget, J.; Bourson, J.; Valeur, B. *J. Lumin.* **1985**, *33*, 273−300.

(21) (a) Förster, T. *Ann. Phys.* **1948**, *2*, 55. (b) Förster, T. *Z. Naturforsch., A* **1949**, *4*, 321. (c) Wieb Van Der Meer, B.; Coker, G., III; Simon Chen, S.-Y. *Resonance Energy Transfer, Theory and Data*; VCH: Weinheim, 1994.

(22) Scholes, G. D.; Harcourt, R. D.; Ghiggino, K. P. *Chem. Phys.* **1995**, *102*, 9574−9581.

(23) Dexter, D. L. *J. Chem. Phys.* **1953**, *21*, 836−850.

(24) (a) Krueger, B. P.; Scholes, G. D.; Fleming, G. R. *J. Phys. Chem. B* **1998**, *102*, 5378−5386. (b) Krueger, B. P.; Scholes, G. D.; Fleming, G. R. *J. Phys. Chem. B* **1998**, *102*, 9603.

theory. The neglect of orbital overlap effects is further justified by the estimated average donor−acceptor separations (vide infra).

To evaluate the ability of Förster theory to describe the systems at hand, it is necessary to compare theoretical and observed energy-transfer rate constants. From Förster theory, the rate constant for energy transfer is given by the equation

$$k_{ET} = 9000(\ln 10)\kappa^2\phi_D J/128\pi^5 n^4 N\tau_D R^6 \qquad (1)$$

where κ^2 is the orientation factor (related to the relative orientation of the donor and acceptor transition dipole moments), ϕ_D is the donor quantum yield in the absence of the acceptor, J is the overlap integral, n is the index of refraction of the solvent, N is Avogadro's number, τ_D is the donor lifetime in the absence of the acceptor, and R is the interchromophoric distance (in cm). The overlap integral J (cm^6/mol) is given by

$$J = \int f_D(\nu)\epsilon_A(\nu)\nu^{-4}\,d\nu \qquad (2)$$

where $f_D(\nu)$ is the fluorescence intensity of the donor, $\epsilon_A(\nu)$ is the molar extinction coefficient of the acceptor, and the integral is calculated over the whole spectrum with respect to the frequency expressed in wavenumbers. This integral represents the overlap between the donor emission spectrum and the acceptor absorption spectrum and is closely related to the probability of energy transfer from the donor to the acceptor. In our calculations, κ^2 is given a value of 2/3, which corresponds to the average over all possible orientations, since the relative alignment of chromophoric dipoles in the dendrimers can be assumed to be random due to the flexible nature of the dendritic backbone.

To calculate the theoretical k_{ET} values, it was necessary to determine the interchromophoric distances within each dendrimer generation. Since the dendrimers are not crystalline, the required distances had to be estimated from molecular modeling. Due to the flexibility of the dendrimers, it is reasonable to assume that, in solution, a wide variety of conformations can be adopted by these relatively large molecules. Additionally, due to the symmetry of the structures, the average distance from the acceptor to any one of the donors should remain constant within a generation when averaging over all the possible conformations. Clearly, a simple minimization representing an arbitrary "snapshot" of the dendrimer structure cannot produce an adequate model from which the required distances can reliably be extracted. Hence, we chose to perform a conformational search on the dendritic structures in which the dihedral angles of the benzylic bonds at each generation within a dendrimer were rotated into the low-energy gauche and anti conformations (120° rotations), and short energy minimizations were performed at each rotation.[25] For instance, in G-2, seven benzylic bonds were rotated to 60, 180, and 300° to produce a total of 2187 different conformations. As expected, the distribution of distances remained relatively constant for all donor−acceptor pairs at each generation, and the average value of all the measured distances was used for the Förster calculation. It should be noted that all of these computer simulations were done in the absence of any solvent molecules, and that the number of rotations of the benzylic bonds, as well as the extent of energy minimization at each rotation was severely limited by the processor speed. Although more thorough calculations would be desirable, the incorporation of additional parameters would unreasonably augment the required calculation time. While the calculated donor−acceptor distances obtained using this approach are not exact, they are consistent with previous estimates and measurements of dendrimer dimensions.[26]

Table 5. Comparison of the Observed and Theoretical Energy-Transfer Rate Constants (k_{ET}) for the Dendrimer Series **1**−**4**

compd	J (D−A) ($\times 10^{14}$ mol^{-1} cm^6)	D−A distance (Å)	k_{ET} ($\times 10^{-10}$) theor	obsd
1	8.06	11.7	65.7	≥3.33[a]
2	8.06	13.6	27.5	≥3.33[a]
3	8.06	14.3	19.9	≥3.33[a]
4	8.06	17.8	5.34	2.00[b]

[a] From time-resolved data based on 30 ps rise time. [b] From time-resolved data based on 50 ps rise time.

The observed energy-transfer rate constants can be calculated using the following relationship:

$$k_{ET} = \frac{1}{\tau_D}\left(\frac{1}{(1/\phi_{ET}) - 1}\right) \qquad (3)$$

where τ_D is the donor fluorescence lifetime in the absence of the acceptor (Table 3, parts c and d) and ϕ_{ET} is the energy-transfer efficiency (Table 4). Since it was found that the fluorescence decays were not monoexponential (vide supra), τ_D was approximated using the average observed lifetime (Table 3, parts c and d).

Table 5 lists the calculated overlap integral, donor−acceptor distance, and theoretical k_{ET} and observed k_{ET} values from time-resolved data. Unfortunately, it is only possible to present the lower limits of the observed k_{ET} values since the exact rate of energy transfer was too fast to be determined using the time-correlated single-photon-counting method. It should again be noted that k_{ET} values are expected to be significantly higher than the limits that are presented, particularly in the lower generations. When this is taken into consideration, the observed values are not in contradiction to those calculated. Additionally, one cannot ignore the fact that the disregard for solvent effects in the molecular modeling will cause error in the determination of donor−acceptor distances. It is expected that inclusion of an appropriate solvent shell around the dendrimers in the computer simulations would expand the dendrimer structure, making the donor−acceptor distances slightly larger. Since the energy-transfer rate constant is proportional to $1/R$,[6] even a small increase in the interchromophoric distance will significantly affect the calculated rate. It is expected that a more sophisticated molecular modeling algorithm along with greater time resolution of the acceptor fluorescence rise will yield much better agreement between the theoretical and observed energy-transfer rate constants.

Finally, it is possible that energy "hopping" from one donor to another along the dendrimer periphery can occur. However, due to the large Stokes shift of coumarin 2, the donor−donor overlap integral (3.74×10^{-16} mol^{-1} cm^6) is 2 orders of magnitude smaller than the donor−acceptor overlap integral (Table 5). This translates to a rate constant for energy transfer that is 2 orders of magnitude slower for donor−donor vs donor−acceptor transfer. As a result, the extent of peripheral energy "hopping" is expected to be minimal, if it occurs at all. Additionally, reverse energy transfer (acceptor to donor) can be ruled out, since the energy difference between the two absorption bands is greater than 6300 cm^{-1}, corresponding to

(25) Either 50 (G-1−G-3) or 100 (G-4) steps of steepest descent energy minimization.

(26) Mourey, T. H.; Turner, S. R.; Rubinstein, M.; Fréchet, J. M. J.; Hawker, C. J.; Wooley, K. L. *Macromolecules* **1992**, *25*, 2401−2406.

rate constants that are 13−14 orders of magnitude slower than for donor to acceptor transfer.

Outlook and Conclusion

The development of nanoscale photonic devices requires the use of a well-defined macromolecular architecture having a large cross section for energy absorption, extremely high quantum yields of fluorescence, good solubility and processability characteristics, and a degree of versatility that allows for the tuning of each of these properties such that the device can be tailored for specific applications. Our approach to the development of laser−dye functionalized dendrimers has allowed us to incorporate highly fluorescent, soluble chromophores into a well-defined macromolecular array. Additionally, by appropriately choosing the chromophores, we have demonstrated that it is possible to achieve almost quantitative through-space energy transfer from the dendrimer periphery to its core. Since the energy-transfer interaction in **1**−**4** is not dependent on the dendrimer backbone structure, additional versatility in our system is possible: the dendrimer framework can be varied to improve features such as processability, rigidity, melting point, UV transparency, reactivity, affinity for guest molecules, etc.

It can be seen from the absorption spectra (Figure 5) that as the number of peripheral chromophores doubles from one dendrimer generation to the next, the amount of absorbed light also doubles. This feature allows the preparation of extremely efficient light-harvesting antenna molecules. Figure 8 indicates that although light is absorbed by the peripheral dyes, emission occurs predominantly from the core dye. Under conditions of constant concentration and illumination intensity, the light output from sensitized excitation of coumarin 343 practically doubles with generation, paralleling the trend in the absorption spectra. Although the quantum yield of energy transfer is high in the molecules studied, it is anticipated that, using this dendrimer framework, the transfer efficiency will drop significantly beyond the fourth generation as a result of increased interchromophoric distance. As dendrimer size continues to increase, an eventual limit will be reached at which light emission from the core will no longer increase with generation and may even decrease.

The dendrimer series **1**−**4** contain both donor and acceptor chromophores. The presence of both dyes in the dendrimer imparts an absorption cross section that spans a wide range (>150 nm). However, due to the efficiency of energy transfer, a photon of any wavelength in this absorption range that is captured by any one of the numerous spatially separated chromophores is transformed into an emitted photon that spans only the narrow emission range for the core dye and emanates from a single point in the macromolecule. Hence, the dendrimers function as both *spectral and spatial* energy concentrators.

The calculation of theoretical energy-transfer rate constants based on Förster theory resulted in values that are 1 order of magnitude higher than those observed. However, the discrepancy in these results is easily explained by considering that it was only possible to determine lower limits of the k_{ET} values, and the actual values are expected to be larger than those reported. Hence, our results are consistent with a Coulombic energy-transfer mechanism and it is expected that further studies involving fluorescence up-conversion experiments to accurately resolve the acceptor rise-time and energy-transfer rate constant, as well as more sophisticated molecular modeling, in which solvent effects would be taken into account, should lead to better agreement between theoretical and observed k_{ET} values in these dendrimers.

Experimental Section

All solvents used for absorption and fluorescence measurements were spectroscopic grade. All measured solutions were degassed by bubbling dry argon through the solution for 5 min. immediately prior to measurement. Absorption spectra (maximum OD <0.1) were recorded on a Uvicon 933 spectrophotometer. Extinction coefficients were calculated over a wide concentration range and were found to remain constant up to an optical density of at least 0.6. The same samples and cuvettes (1 cm^2) were used to directly record the emission and excitation spectra on an ISA/SPEX Fluorolog 3.22 equipped with a 450 W Xe lamp, double-excitation and double-emission monochromators, and a digital photon-counting photomultiplier. Slit widths were set to 1.3 nm band-pass on both excitation and emission. Correction for variations in lamp intensity over time and λ was achieved using a reference silicon photodiode. The spectra were further corrected for variations in photomultiplier response over λ and for the path difference between the sample and the reference by multiplication with emission and excitation correction curves generated on the instrument. Quantum yields of fluorescence were obtained by comparing the integrated fluorescence spectra to the fluorescence spectrum of quinine sulfate in 1.0 N H_2SO_4 ($\Phi_F = 0.55$),[27] and all measurements were corrected for refractive index differences relative to water.[28] The photostability of the dye-labeled dendrons was ascertained by monitoring the emission intensity of the central dye under irradiation at the λ_{max} of the peripheral chromophores: no photodegradation could be detected after 1 h of irradiation. MALDI-TOF mass spectrometry was performed on a Perseptive Biosystems Voyager-DE spectrometer using delayed extraction mode and with an acceleration voltage of 20 keV. Samples were prepared by using a 1:20 ratio of analyte (5 mg/mL in THF) to matrix solution (*trans*-indoleacrylic acid, 10 mg/mL in THF).

Fluorescence decay measurements were made with the time-correlated single-photon-counting method as described previously.[6c,29] Briefly, a Ti:sapphire regenerative amplifier (Coherent RegA 9050) operating at 250 kHz was used to pump an optical parametric amplifier (Coherent OPA 9450). The 340 nm second harmonic of OPA output was used as the excitation light source and was attenuated to less than 1 mW at the sample, which was contained in a 1 cm^2 cuvette equipped with a magnetic stirrer. The fluorescence from the sample was separated from the scattering excitation light with a cutoff filter and spectrally separated with a monochromator. The fluorescence signal was detected with a multichannel plate photomultiplier. The instrument response functions were measured using a scattering solution (nondairy creamer). We typically obtained 80 ps for the fwhm of the instrument function. The fluorescence decay curves were fitted to a sum of exponentials by using the nonlinear least-squares method. Samples were prepared to give an optical density of ~0.1 at 340 nm. Fluorescence decays were observed at either 420 nm (for **5**−**9**) or at 470 nm (for **1**−**4**), and all measurements were taken at magic angle (54.7°) polarization.

HPLC analysis was performed using a Phenomenex UK reversed-phase C_{18} column at a flow rate of 1.2 mL/min. The solvent compostion consisted of CH_3CN (solvent A)/THF (solvent B) using the gradient table given below:

gradient	time (min)	flow (mL/min)	% A	% B
1		1.20	41.0	59.0
2	3.00	1.20	41.0	59.0
3	8.00	1.20	21.0	70.0
4	14.00	1.20	21.0	79.0

All chromatographic separations were performed at room temperature using Waters M510 and M501 pumps, a Waters M717 autosampler, and a Waters M996 UV photodiode array detector (scanned range was 240−500 nm).

Molecular modeling was done on a Silicon Graphics workstation equipped with Molecular Simulations Inc. (MSI) Insight II software. All structures were initially optimized using 1000−10 000 steps (depending on dendrimer generation) of steepest descent energy minimization in the Discover module's cvff force field with the dielectric constant set to 1.00. Once the minimization was complete, the benzylic bonds were rotated using the Rotors function of the

Discover module with a starting angle of 60°, a rotation angle of 240°, and two intervals (forcing dihedral angles of 60, 180, and 300°). At each rotation, 50−100 steps of steepest descent energy minimization were executed, eliminating any drastically high energy conformations resulting from the rotations. To restrict the total calculation time to a realistic value, only seven bonds were rotated in any one calculation for the third- and fourth-generation dendrimers. All different seven-bond combinations were used in order to gain adequate values for the desired distances in these generations.

Acknowledgment. This research was supported by the AFOSR MURI program and the Department of Energy (LBNL Contract DE-AC03-76SF00098). We gratefully acknowledge the help of Nikolay Vladimirov with the HPLC analysis of the dendrimers, and Kathy Durkin for many helpful discussions about the molecular modeling. A.A. and K.O. thank the Eastman Kodak Co. and the Japan Society of Promotion for Science for Young Scientists for respective fellowship support.

JA993272E

(27) Demas, J. N.; Crosby, G. A. *J. Phys. Chem.* **1971**, *75*, 991−1024.
(28) Ediger, M. D.; Moog, R. S.; Boxer, S. G.; Fayer, M. D. *Chem. Phys. Lett.* **1982**, *88*, 123−127.
(29) Chang, M. C.; Courtney, S. H.; Cross, A. J.; Gulotty, R. J.; Petrich, R. J.; Fleming, G. R. *Anal. Instrum.* **1985**, *14*, 433−464.